Preprints of the 21st IFAC World Congress (Virtual)
Berlin, Germany, July 12-17, 2020

Dual multi-stage NMPC using sigma point principles ⋆

Sakthi Thangavel * **Radoslav Paulen** ** **Sebastian Engell** *

* *Process Dynamics and Operations Group, Technische Universität Dortmund, Emil-Figge-Straße 70, 44227 Dortmund, Germany (e-mail: sakthi.thangavel@tu-dortmund.de)*
** *Faculty of Chemical and Food Technology, Slovak University of Technology in Bratislava, Radlinského 9, 812 37 Bratislava, Slovakia*

Abstract: Dual control is a technique that addresses the trade-off between probing (excitation signals) and control actions, which results in a better estimation of the unknown parameters and therefore in a better (tracking or economic) performance. Multi-stage NMPC is a robust-control scheme that represents the uncertainty using a scenario tree that is often built by assuming parametric uncertainty and by taking into account the minimum, nominal and maximum values of the uncertain parameters. If the uncertainty set is not a box, this procedure augments the uncertainty set and results in a loss of performance. Here, we mitigate this problem by tightly approximating the uncertainty set using the so-called sigma points and computing an ellipsoidal over-approximation of the reachable set of the system using the unscented transformation. We also improve the performance by considering the future reduction of the ranges of the uncertainties due to control actions and measurements thereby achieving implicit dual control actions. The advantages of the proposed approach over the standard multi-stage NMPC scheme are demonstrated for a linear and a nonlinear (semi-batch reactor) simulation case study.

Keywords: Adaptive control, dual control, parameter uncertainty, robust model predictive control, multi-stage NMPC, parametric uncertainty, unscented transformation

1. INTRODUCTION

The control of dynamic systems under uncertainty is one of the major research topics in the control community. In the scope of model predictive control (MPC), several robust MPC strategies exist to handle model uncertainties and to control MIMO systems while adhering to constraints (Scokaert and Mayne, 1998; Mayne et al., 2005; Lucia et al., 2013). Such schemes necessarily introduce some conservatism (loss of performance) when compared to the situation when the true plant model is known. Among the several robust MPC schemes, multi-stage MPC considers future recourse actions on a scenario tree of discrete-valued uncertainties and is able to provide the closed-loop optimal solution if the assumption on the uncertainty model is correct. It is therefore less conservative compared to other robust approaches for general non-linear systems (see e.g. Lucia et al. (2012, 2013)). Several variants of the multi-stage NMPC exist in literature (Thangavel et al., 2018a,b,c, 2019).

The performance of the robust controllers can be improved using adaptive approaches (Wittenmark, 1995; Thangavel et al., 2018a), where the plant measurements are used to improve the knowledge about the plant by reducing the uncertainty. However, uncertainty always exists in the parameter estimates due to the presence of noise in the measurements. This uncertainty is commonly represented by a confidence region of the parameter estimates which can be computed approximately using the Fisher information matrix and has the shape of an ellipsoid (Franceschini and Macchietto, 2008; Bargiela, 2001). When generating the scenario tree of the the multi-stage MPC, this ellipsoid is often over-approximated by a box which can increase the conservatism and decrease the performance. This problem can be mitigated by borrowing ideas from the unscented transformation (Julier and Uhlmann, 1997). Open-loop robust control schemes based on unscented transformation where presented in Heine et al. (2006); Völz and Graichen (2015), but they do not take into account the presence of future feedback information hence these approaches are conservative when compared to closed-loop schemes (Scokaert and Mayne, 1998; Farrokhsiar and Najjaran, 2012). The feedback information can be taken into account by embedding the unscented Kalman filter equations into the NMPC optimization problems, resulting in computationally intensive optimization problems (Yan and Bitmead, 2005; Farrokhsiar and Najjaran, 2012).

A novel computationally efficient closed-loop robust multi-stage NMPC strategy using the unscented transformation was developed in Thangavel et al. (2020a). The scenario tree is generated for a finite number of points that are chosen from the uncertainty set, called the sigma points (Wan

⋆ The authors acknowledge the German Academic Exchange Service (DAAD) and The Ministry of Education, Science, Research and Sport of the Slovak Republic under the Exchange Involving Project "Reliable and Real-time Feasible Estimation and Control of Chemical Plants". RP acknowledges the contribution of the Slovak Research and Development Agency (project APVV 15-0007) and of the European Commission (grant 790017).

and Van Der Merwe, 2000), which tightly approximate the uncertainty set. The state covariance matrix is computed from the predictions that are obtained using the different realizations of the uncertain parameters according to the sigma points. The state covariance matrix is scaled using a tuning parameter such that the reachable set (the predictions obtained from all the realizations of the uncertainty within the uncertainty set) is contained in an ellipsoidal set. This eliminates the need of embedding the unscented Kalman filter equations into the optimization problem. An adaptive variant of the multi-stage NMPC using sigma point principles which uses the plant measurement to reduce the uncertainty and further enhance the performance has been introduced in Thangavel et al. (2020b).

The information obtained from the system can be improved by providing excitation signals (probing actions) to the plant, which results in smaller parametric confidence regions. However, the probing actions may deteriorate the closed-loop performance of the system. There exists a trade-off between the probing actions, which give a better estimate of the uncertain parameters, and the optimizing control input, which results in the best achievable closed-loop performance. This was discussed for the first time as *dual* control in Feldbaum (1960). Dual control poses a very challenging problem, which is in general computationally intractable and can only be solved by introducing some approximations. Dual control schemes are broadly classified into implicit and explicit schemes (Filatov and Unbehauen, 2000). Explicit controllers consider the effect of the control actions on the model uncertainty by an additional term in the cost function whereas the implicit controllers take the effect of the probing actions on the overall performance into account (Mesbah, 2018).

In this paper, we propose a robust implicit dual nonlinear MPC (NMPC) formulation in the framework of multi-stage NMPC based on sigma point principles. The dual scheme considers the predictions obtained from the sigma points to be the future measurements, predicts the future confidence regions and updates the scenario tree of the multi-stage NMPC accordingly. This helps the proposed scheme to take into account the impact of the future probing actions on the overall performance of the controller and results in an implicit dual control action. The advantages of the proposed dual approach over the adaptive and the standard multi-stage NMPC scheme are demonstrated for a linear and for a nonlinear (semi-batch reactor) simulation case study.

The remainder of this paper is organized as follows. The problem statement and the unscented transformation are explained in section 2. Section 3 describes the traditional multi-stage NMPC scheme. Section 4 introduces multi-stage NMPC using sigma point principles. Section 5 and section 6 explains adaptive multi-stage NMPC and the proposed dual multi-stage NMPC scheme using sigma point principles. Section 7 presents the results obtained using different robust NMPC strategies for a linear case study and a benchmark nonlinear semi-batch reactor example. Finally, the paper is concluded in section 8.

2. PRELIMINARIES

The nominal model of the plant is given as

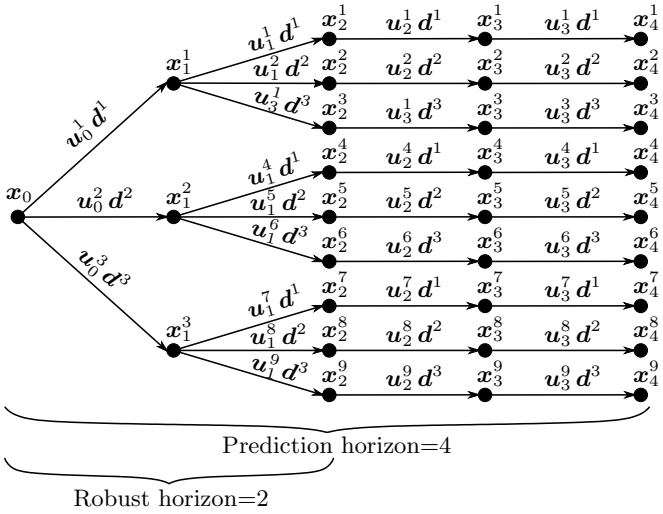

Fig. 1. Scenario tree of the multi-stage NMPC.

$$\boldsymbol{x}_{k+1} = \boldsymbol{f}(\boldsymbol{x}_k, \boldsymbol{u}_k, \boldsymbol{d}), \tag{1}$$

where $\boldsymbol{x} \in \mathbb{R}^{n_x}$, $\boldsymbol{u} \in \mathbb{R}^{n_u}$ and $\boldsymbol{d} \in \mathbb{R}^{n_d}$ represent the plant state variables, control inputs and time invariant uncertain model parameters, respectively. All the states are assumed to be measured. The plant measurements are assumed to be corrupted by white Gaussian noise. The exact values of the model parameters are not known, but they are known to be contained in an ellipsoidal set. The ellipsoidal set is parameterized by the nominal parameter $\boldsymbol{d}_0$ (center) and its parameter covariance matrix $\boldsymbol{P}_0$ and is given as

$$\mathbb{D}(\boldsymbol{d}_0, \boldsymbol{P}_0) := \{\boldsymbol{d} \in \mathbb{R}^{n_d} | (\boldsymbol{d} - \boldsymbol{d}_0)^T \boldsymbol{P}_0^{-1} (\boldsymbol{d} - \boldsymbol{d}_0) \leq 1\}. \tag{2}$$

The set is assumed to form a finite support of the probability distribution of the model parameters. The unscented transformation is used to compute the statistics of random variables which undergo a nonlinear transformation (Julier and Uhlmann, 1997). Here, it is employed to compute the ellipsoidal approximation of the reachable set of the system (1). The sigma points are chosen such that they capture the true mean and covariance of the uncertainty set $\mathbb{D}$ and are given as

$$\mathbb{S}(\boldsymbol{d}_0, \boldsymbol{P}_0) = \boldsymbol{d}_0 \cup \left(\bigcup_{i=1}^{n_d} \boldsymbol{d}_0 - \boldsymbol{P}_{0,[i,\star]}^{\frac{1}{2},T} \right) \cup \left(\bigcup_{i=1}^{n_d} \boldsymbol{d}_0 + \boldsymbol{P}_{0,[i,\star]}^{\frac{1}{2},T} \right), \tag{3}$$

where $\boldsymbol{P}_{0,[i,\star]}^{\frac{1}{2}}$ represents the transpose of the i^{th} row vector of the Cholesky factor of $\boldsymbol{P}_0$. The chosen $2n_d + 1$ sample points are propagated through the nonlinear function $\boldsymbol{f}(\cdot)$ to compute the state mean ($\boldsymbol{x}_{m,k+1}$) and state covariance matrix ($\boldsymbol{X}_{c,k+1}$) as given below

$$\boldsymbol{x}_{k+1}^i = \boldsymbol{f}(\boldsymbol{x}_k, \boldsymbol{u}_k, \boldsymbol{d}^i), \quad \boldsymbol{d}^i \in \mathbb{S}(\boldsymbol{d}_0, \boldsymbol{P}_0), \quad \forall i \in \mathcal{I}_1, \tag{4a}$$

$$\boldsymbol{x}_{m,k+1} = \textstyle\sum_{i=1}^{2n_d+1} v_i \boldsymbol{x}_{k+1}^i, \quad \textstyle\sum_{i=1}^{2n_d+1} v_i = 1, \tag{4b}$$

$$\boldsymbol{X}_{c,k+1} = \kappa^2 \textstyle\sum_{i=1}^{2n_d+1} v_i \, \boldsymbol{x}_{c,k+1}^i \boldsymbol{x}_{c,k+1}^{i,T}, \tag{4c}$$

where $\boldsymbol{x}_{c,k+1}^i = \boldsymbol{x}_{k+1}^i - \boldsymbol{x}_{m,k+1}$, $\mathcal{I}_1 := \{1, \cdots, 2n_d + 1\}$, v_i is the weight associated with each sigma point, and $\kappa \in \mathbb{R}$ is the scaling factor of the state covariance matrix.

3. MULTI-STAGE NMPC (MS NMPC)

Multi-stage NMPC (MS NMPC) models the uncertainty about the true plant dynamics by a tree of discrete scenarios as shown in Fig. 1. Each branch in the scenario

tree represents a particular realization of the uncertain parameters. The future control inputs are computed while taking into account that measurement information will be available in the future, and so the control moves can be adapted accordingly. This provides a closed-loop control formulation and results in better performance when compared to the traditional open-loop min-max approaches (Lucia et al., 2012). In the presence of continuous valued uncertainties a scenario tree that is generated for all combinations of the minimum, nominal and maximum values of the uncertain parameters usually provides a good approximation of the uncertainty set $\mathbb{D}$ (Lucia et al., 2013).

The receding horizon problem solved at time t reads as:

$$\min_{\boldsymbol{x}_k^j, \boldsymbol{u}_k^j \forall (j,k) \in \mathcal{I}_2, \boldsymbol{d}_k^j \in \mathcal{D}_k^j} \quad J_1 + J_3, \tag{5a}$$

subject to

$$\boldsymbol{x}_{k+1}^j = \boldsymbol{f}(\boldsymbol{x}_k^{p(j)}, \boldsymbol{u}_k^j, \boldsymbol{d}_k^{r(j)}), \quad \forall\, (j, k+1) \in \mathcal{I}_2, \tag{5b}$$

$$\boldsymbol{g}(\boldsymbol{x}_{k+1}^j, \boldsymbol{u}_k^j) \leq 0\,, \quad \forall\, (j, k+1) \in \mathcal{I}_2, \tag{5c}$$

$$\boldsymbol{u}_k^j = \boldsymbol{u}_k^l \text{ if } \boldsymbol{x}_k^{p(j)} = \boldsymbol{x}_k^{p(l)}, \quad \forall\, (j,k), (l,k) \in \mathcal{I}_2, \tag{5d}$$

$$\underline{\boldsymbol{d}}_0 = \boldsymbol{d}_0 - \text{diag}^{\frac{1}{2}}(\boldsymbol{P}_0), \ \overline{\boldsymbol{d}}_0 = \boldsymbol{d}_0 + \text{diag}^{\frac{1}{2}}(\boldsymbol{P}_0), \tag{5e}$$

$$\mathcal{D}_k^j = \mathbb{A}_1(\underline{\boldsymbol{d}}_0, \boldsymbol{d}_0, \overline{\boldsymbol{d}}_0), \quad \forall (j,k) \in \mathcal{I}_2, \tag{5f}$$

where $\text{diag}^{\frac{1}{2}}(\cdot)$ gives the element-wise square root of the main diagonal of a matrix. The set of indices (j,k) that occur in a given scenario tree is denoted by $\mathcal{I}_2$. The state vector $\boldsymbol{x}_{k+1}^j$ at stage $k+1$ and position j in the scenario tree is obtained using the parent state $\boldsymbol{x}_k^{p(j)}$, the control input $\boldsymbol{u}_k^j$ and the uncertainty realization $\boldsymbol{d}^{r(j)} \in \mathcal{D}_k^j$. The set $\mathcal{D}_j^k$ contains the set of all possible combinations of the minimal ($\underline{\boldsymbol{d}}_0$), nominal ($\boldsymbol{d}_0$) and maximal ($\overline{\boldsymbol{d}}_0$) value of the uncertainty set $\mathbb{D}$. $\mathbb{A}_1(\cdot)$ generates a set which contains all possible parameter combinations obtained using the minimal, nominal and maximal value of the uncertain parameters. This results in 3^{n_d} branches to be considered at each node in the scenario tree. The size of the tree grows exponentially along the prediction horizon (of the length N_p), which can be avoided by assuming that the uncertainty remains constant after the so-called robust horizon (N_r). The robust horizon is chosen such that it provides a trade-off between the numerical complexity and the representation of all possible evolutions. The objective function (5a) is defined (using J_1 and J_3) as

$$J_1 = \sum_{k=t}^{t+N_r-1} \sum_{j=1}^{N_b{}^{k+1}} \omega_{k+1}^j L(\boldsymbol{x}_{k+1}^j, \boldsymbol{u}_k^j), \tag{6a}$$

$$J_3 = \sum_{k=t+N_r}^{t+N_p-1} \sum_{j=1}^{N_b{}^{N_r}} \omega_{k+1}^j L(\boldsymbol{x}_{k+1}^j, \boldsymbol{u}_k^j), \tag{6b}$$

where N_b and $L(\cdot)$ represent the number of branches and cost at each node in the scenario tree, respectively. J_1 gives the accumulated cost of all nodes until the robust horizon, and J_3 gives the accumulated cost of all nodes after the robust horizon until the end of the prediction horizon. ω_k^j is the weight associated with each node in the scenario tree and is chosen as given below, where $\mathcal{I}_3 := \{1, \cdots, N_r\}$, and $\mathcal{I}_4 := \{N_r+1, \cdots, N_p\}$:

$$\sum_{j=1}^{N_b{}^k} \omega_k^j = 1, \ \forall k \in \mathcal{I}_3, \quad \sum_{j=1}^{N_b{}^{N_r}} \omega_k^j = 1, \ \forall k \in \mathcal{I}_4. \tag{7}$$

The additional constraints that are imposed at each node in the scenario tree are given by (5c). The non-anticipativity constraints (5d) make sure that the control decisions taken with the same information are equal (i.e., in Fig. 1, $\boldsymbol{u}_0^1 = \boldsymbol{u}_0^2 = \boldsymbol{u}_0^3; \boldsymbol{u}_1^1 = \boldsymbol{u}_1^2 = \boldsymbol{u}_1^3; \dots$).

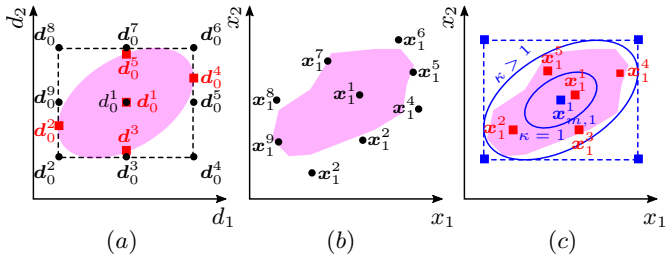

Fig. 2. Comparison between MS NMPC and the proposed MS-SP NMPC. (a) parameter confidence region, (b) reachable set of model (1), (c) ellipsoidal over-approximation of the reachable set of model (1).

4. MULTI-STAGE NMPC USING SIGMA POINT PRINCIPLES (MS-SP NMPC)

The scenario tree of multi-stage NMPC using sigma point principles is built using $2n_d+1$ sample points chosen from the uncertainty set known as the sigma points (Thangavel et al., 2020a). The basic idea is to *over-approximate the reachable set* of the model (1) using the scaled unscented transformation (Julier, 2002). The sigma points are chosen in the parametric space and are propagated through the nonlinear model to obtain the state covariance matrix w.r.t. the uncertainty along with its mean using (4). The objective and the constraint functions of multi-stage NMPC using sigma point principles (MS-SP NMPC) are evaluated over the box over-approximation of the reachable set described by the state mean and the state covariance matrix.

The key difference between standard MS NMPC (Section 3) and MS-SP NMPC is shown in Fig. 2 for a system with two states, two uncertain parameters and a given control input at time $k = 0$. The pink shaded region in Fig. 2(a) represents the confidence region of the uncertain parameters, the black dots and the red squares are the samples chosen to build the scenario tree of MS and MS-SP NMPC, respectively. The pink shaded region in Figs. 2(b)–(c) represents the corresponding reachable set of the states given the model (1). The black circles in Fig. 2(b) and the red squares in Fig. 2(c) represent the state predictions obtained on the branches of the scenario tree of MS and MS-SP NMPC, respectively. The inner (blue) ellipsoid represents the ellipsoidal approximation of the reachable set of the model (1) described by the state mean and the unscaled state covariance matrix (i.e. $\kappa = 1$ in (4c)). The covariance matrix is scaled using the factor κ such that the extended ellipsoidal set over-approximates the reachable set and is represented by the outer (blue) ellipsoid. Blue squares represent the state mean and the vertices of the box over-approximation of the ellipsoidal over-approximation of the reachable set for which the objective and constraint functions of MS-SP NMPC are evaluated. The proposed MS-SP NMPC considers the entire reachable set of the states, which does not need to be the case in general for the scenario tree of standard MS NMPC. The scenario tree of standard MS NMPC grows exponentially with respect to the number of uncertain

parameters where as the scenario tree of the MS-SP NMPC grows linearly in this respect.

The proposed MS-SP NMPC optimization problem that is solved at time t reads as follows, where $N_b = 2n_d + 1$, $\mathcal{I}_6(k) := \{1, \cdots, N_b^{k-1}\}$, $s = (r-1)N_b + i$ and $\boldsymbol{x}_{c,k}^s = \boldsymbol{x}_k^s - \boldsymbol{x}_{m,k}^r$.

$$\min_{\boldsymbol{x}_k^j, \boldsymbol{u}_k^j \forall (j,k) \in \mathcal{I}, \boldsymbol{d}_k^j \in \mathcal{D}_k^j} \quad J_2 + J_3, \tag{8a}$$

subject to: (5b), (5c), (5d), $\forall (j, k+1) \in \mathcal{I}_5$,

$$\mathcal{D}_k^j = \mathbb{S}(\boldsymbol{d}_0, \boldsymbol{P}_0), \qquad \forall (j,k) \in \mathcal{I}_5, \tag{8b}$$
$$\boldsymbol{x}_{m,k}^r = \textstyle\sum_{i=1}^{N_b} v_i \, \boldsymbol{x}_k^s, \qquad \forall k \in \mathcal{I}_3, r \in \mathcal{I}_6(k), \tag{8c}$$
$$\boldsymbol{X}_{c,k}^r = \kappa^2 \textstyle\sum_{i=1}^{N_b} v_i \, \boldsymbol{x}_{c,k}^s \boldsymbol{x}_{c,k}^{s,T}, \qquad \forall k \in \mathcal{I}_3, r \in \mathcal{I}_6(k), \tag{8d}$$
$$\underline{\boldsymbol{x}}_{m,k}^r = \boldsymbol{x}_{m,k}^r - \mathrm{diag}^{\frac{1}{2}}(\boldsymbol{X}_{c,k}^r), \qquad \forall k \in \mathcal{I}_3, r \in \mathcal{I}_6(k), \tag{8e}$$
$$\overline{\boldsymbol{x}}_{m,k}^r = \boldsymbol{x}_{m,k}^r + \mathrm{diag}^{\frac{1}{2}}(\boldsymbol{X}_{c,k}^r), \qquad \forall k \in \mathcal{I}_3, r \in \mathcal{I}_6(k), \tag{8f}$$
$$\mathcal{X}_k^r = \boldsymbol{x}_{m,k}^r \cup \mathbb{A}_2(\underline{\boldsymbol{x}}_{m,k}^r, \overline{\boldsymbol{x}}_{m,k}^r), \quad \forall k \in \mathcal{I}_3, r \in \mathcal{I}_6(k), \tag{8g}$$
$$\boldsymbol{g}(\boldsymbol{x}, \boldsymbol{u}_{k-1}^{(r-1)N_b+1}) \leq 0\,, \quad \forall k \in \mathcal{I}_3, r \in \mathcal{I}_6(k), x \in \mathcal{X}_k^r. \tag{8h}$$

The scenario tree of MS-SP NMPC considers $2n_d + 1$ branches at each node. $\mathcal{I}_5$ represents the set of all occurring indices in the scenario tree. $\boldsymbol{X}_{c,k}^r$ represents the state covariance matrix that is obtained while applying control input $\boldsymbol{u}_{k-1}^{(r-1)N_b+1}$ at the parent state $\boldsymbol{x}_{k-1}^{\lceil r/N_b \rceil}$, where $\lceil \cdot \rceil$ represents the ceil operator. Referring to Fig. 1, $\boldsymbol{X}_{c,2}^2$ is computed using the state predictions $\boldsymbol{x}_2^4$, $\boldsymbol{x}_2^5$ and $\boldsymbol{x}_2^6$ that were obtained from the parent state $\boldsymbol{x}_1^2$ when the control input $\boldsymbol{u}_1^4$ ($\boldsymbol{u}_1^4 = \boldsymbol{u}_1^5 = \boldsymbol{u}_1^6$ due to non-anticipativity constraints) is applied. The state covariance matrix is scaled such that all reachable states are covered using a scaling factor κ which is a tuning parameter. The lower and upper bounds on the state predictions can be obtained using (8e) and (8f). The set of all possible combinations of the lower and upper bounds on the state predictions (given by $\mathbb{A}_2(\cdot)$) along with the center of the state ellipsoid is obtained in (8g). The constraint functions $\boldsymbol{g}(\cdot)$ are satisfied for the vertices of the box over-approximation of the predicted state ellipsoids using (8h). This guarantees robust constraint satisfaction if

$$\max_{\boldsymbol{x} \in \mathcal{X}_k^r} \boldsymbol{g}(\boldsymbol{x}, \boldsymbol{u}_{k-1}^{(r-1)N_b+1}) \geq \max_{\boldsymbol{x} \in \mathbb{X}_k^r} \boldsymbol{g}(\boldsymbol{x}, \boldsymbol{u}_{k-1}^{(r-1)N_b+1}), \tag{9}$$

is satisfied. $\mathbb{X}_k^r$ represents the reachable set of model (1). The scaling factor κ should be chosen such that the condition (9) is satisfied (κ determines the elements of the set $\mathcal{X}_k^r$). The scaling factor κ can be obtained by solving an optimization problem such that it satisfies (9) for the cases where the sensitivity of the constraints w.r.t. the state does not change its sign as shown in Thangavel et al. (2020a).

The objective function of the proposed scheme is given in (8a), where J_2 is given as

$$J_2 = \textstyle\sum_{k=0}^{N_r-1} \sum_{r=1}^{N_b{}^k} \sum_{j=1}^{2n_x+1} \omega_{k+1}^{j+r-1} L(\boldsymbol{x}^j, \boldsymbol{u}_k^{(r-1)N_b+1}), \tag{10}$$

where $\boldsymbol{x}^j$ represents the j^{th} element of the set $\mathcal{X}_{k+1}^r$. ω_k^{j+r-1} is the weight associated with $\boldsymbol{x}^j$ and is chosen s.t.

$$\textstyle\sum_{r=1}^{N_b{}^{k-1}} \sum_{j=1}^{2^{n_x}+1} \omega_k^{j+r-1} = 1, \forall k \in \mathcal{I}_3. \tag{11}$$

5. ADAPTIVE MULTI-STAGE NMPC USING SIGMA POINT PRINCIPLES (A-MS-SP NMPC)

Adaptive control (following the certainty-equivalence approach) uses the information that is available from the plant measurements to improve the knowledge about the plant dynamics, thereby improving the closed-loop performance of model-based controllers. The measurements can be used to estimate the uncertain parameters $\tilde{\boldsymbol{d}}_t$ e.g., using least-squares estimation (LSE). A confidence region of the parameter estimates can be obtained using the Fisher information matrix $\boldsymbol{F}_t$ (FIM), if we assume that the plant measurements are corrupted by white Gaussian noise (Franceschini and Macchietto, 2008):

$$\boldsymbol{F}_t \approx \textstyle\sum_{k=0}^{t} \boldsymbol{s}_k^T \boldsymbol{Q} \boldsymbol{s}_k, \tag{12}$$

where $\boldsymbol{F}_t$ represents the FIM obtained using the measurements observed from time 0 to t, $\boldsymbol{Q}$ is the inverse of the measurement noise covariance matrix and $\boldsymbol{s}_k = \frac{\partial \boldsymbol{x}_k}{\partial \boldsymbol{d}}|_{\tilde{\boldsymbol{d}}_t}$ represents the sensitivity matrix of the measurements (the states in our case) w.r.t. the parameters.

The FIM can be used to obtain the confidence region of the uncertain parameters which is centered around the least-squares estimate and is given by

$$(\boldsymbol{d} - \tilde{\boldsymbol{d}}_t)^T \boldsymbol{F}_t (\boldsymbol{d} - \tilde{\boldsymbol{d}}_t) \leq n_d \, F_{\text{dist}}(n_d, t - n_d, \alpha), \tag{13}$$

where F_{dist} is a quantile of the Fisher distribution and α stands for the desired confidence level (normally 95% or 99%). It is assumed that the true value of the uncertain parameter is always contained in the confidence region. $\tilde{\boldsymbol{P}}_t$ represents the (Cramer-Rao) upper bound on the parameter covariance matrix with confidence level α.

$$\tilde{\boldsymbol{P}}_t = n_d \, F_{\text{dist}}(n_d, t - n_d, \alpha) \boldsymbol{F}_t^{-1}. \tag{14}$$

The scenario tree of A-MS-SP NMPC is updated whenever new measurement information from the plant becomes available. The underlying optimization problem is the same as (8) but with (8b) being replaced by

$$\check{\boldsymbol{d}} = \boldsymbol{d}_{t-1} - \tilde{\boldsymbol{d}}_t, \quad \check{\boldsymbol{P}} = \phi \boldsymbol{P}_{t-1}^{-1} + (1-\phi) \tilde{\boldsymbol{P}}_t^{-1} \tag{15a}$$
$$\boldsymbol{P}_t = [1 - \phi(1-\phi) \check{\boldsymbol{d}}^T \tilde{\boldsymbol{P}}_t^{-1} \check{\boldsymbol{P}}^{-1} \boldsymbol{P}_{t-1}^{-1} \check{\boldsymbol{d}}] \check{\boldsymbol{P}}^{-1}, \tag{15b}$$
$$\boldsymbol{d}_t = \check{\boldsymbol{P}}^{-1} [\phi \boldsymbol{P}_{t-1}^{-1} \boldsymbol{d}_{t-1} + (1-\phi) \tilde{\boldsymbol{P}}_t^{-1} \tilde{\boldsymbol{d}}_t], \tag{15c}$$
$$\mathcal{D}_k^j = \mathbb{S}(\boldsymbol{d}_t, \boldsymbol{P}_t), \quad \forall (j,k) \in \mathcal{I}_5, \tag{15d}$$

where $\phi \in [0, 1]$ is an additional degree of freedom of the A-MS-SP NMPC optimization problem. The scenario tree is built using an ellipsoidal over-approximation of the intersection of two ellipsoids as in Kurzhanskiy and Varaiya (2006). The first ellipsoid represents the prior information (past confidence region) and the second one is an update based on the measurements up to time t. The intersection operation (15a)–(15c) can be compactly represented as $(\boldsymbol{d}_t, \boldsymbol{P}_t) = \mathbb{I}(\boldsymbol{d}_{t-1}, \tilde{\boldsymbol{d}}_t, \boldsymbol{P}_{t-1}, \tilde{\boldsymbol{P}}_t, \phi)$.

6. DUAL MULTI-STAGE NMPC USING SIGMA POINT PRINCIPLES (D-MS-SP NMPC)

Implicit dual control requires predicting the impact of the probing actions on the uncertainty quantification (parametric confidence regions). This information can then be used to update the scenario tree of MS NMPC over the prediction horizon (Thangavel et al., 2018a). Thangavel et al. (2017) assumed the predictions that are used in the

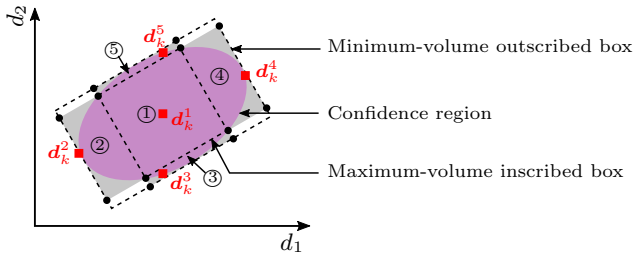

Fig. 3. Box-partition of a confidence region to $2n_d + 1$ boxes. Box ⓙ is considered in scenario j.

branches of the scenario tree to be the predictions of the plant measurements and computed the future parameter estimates and the respective confidence regions by an approximate LSE. It was pointed out in Thangavel et al. (2017) that this approach does not guarantee that the predicted confidence regions enclose the true values of the uncertain parameters thereby comprising the robustness of the approach. Hence, the predicted confidence regions were augmented to take into account the uncertainty in the future parameter estimates and to restore the robustness of the approach. In this paper, we extend this approach to the MS-SP NMPC formulation.

The formulation of D-MS-SP NMPC is similar to the A-MS-SP NMPC optimization problem where (15) is considered only for the first stage (i.e. $\mathcal{D}_0^1$) in the scenario tree and the parameters used to build the rest of the scenario tree are obtained using the following equations, $\forall\,(j, k{+}1) \in \mathcal{I}_7$, where $\mathcal{I}_7$ represents the set of all occurring indices in the scenario tree until $k < t + N_r$.

$$\hat{\boldsymbol{F}}^{j}_{k+1} = \hat{\boldsymbol{F}}^{p(j)}_{k} + \frac{\partial \boldsymbol{x}^{j}_{k+1}}{\partial \boldsymbol{d}^T}\Big|_{\boldsymbol{d}^{r(j)}_k} \boldsymbol{Q} \frac{\partial \boldsymbol{x}^{j}_{k+1}}{\partial \boldsymbol{d}}\Big|_{\boldsymbol{d}^{r(j)}_k}, \tag{16a}$$

$$\tilde{\boldsymbol{d}}^{j}_{k+1} = \hat{\boldsymbol{F}}^{j,-1}_{k+1}(\hat{\boldsymbol{F}}^{p(j)}_{k}\boldsymbol{d}^{p(j)}_{k} + (\hat{\boldsymbol{F}}^{j}_{k+1} - \hat{\boldsymbol{F}}^{p(j)}_{k})\boldsymbol{d}^{r(j)}_{k}), \tag{16b}$$

$$\hat{\mathcal{D}}^{j}_{k+1} := \left\{ \mathbb{T}(\boldsymbol{d}^{p(j)}_{k}, \boldsymbol{P}^{p(j)}_{k}, \boldsymbol{\alpha}, j), \forall \boldsymbol{\alpha} \in \mathbb{R}^{n_d} \middle| \begin{matrix} \|\boldsymbol{\alpha}\|_1 = n_d \\ \|\boldsymbol{\alpha}\|_\infty \leq 1 \end{matrix} \right\}, \tag{16c}$$

$$\mathbb{T}(\cdot) := \begin{cases} \boldsymbol{d}^{p(j)}_{k} - \sqrt{\boldsymbol{P}^{p(j)}_{k}}\,(\boldsymbol{c}^{j} + \boldsymbol{T}^{j}\boldsymbol{\alpha}), & \text{if } j \leq n_d + 1 \\ \boldsymbol{d}^{p(j)}_{k} + \sqrt{\boldsymbol{P}^{p(j)}_{k}}\,(\boldsymbol{c}^{j-n_d} + \boldsymbol{T}^{j}\boldsymbol{\alpha}), & \text{otherwise} \end{cases}, \tag{16d}$$

$$c^{a}_{[i]} := \begin{cases} \frac{\sqrt{n_d}+1}{2\sqrt{n_d}}, & \text{if } i = a-1 \\ 0, & \text{otherwise} \end{cases}, T^{a}_{[i,l]} := \begin{cases} \frac{\sqrt{n_d}-1}{2\sqrt{n_d}}, & \text{if } a-1 = i = l \\ \frac{1}{\sqrt{n_d}}, & \text{if } i = l \\ 0, & \text{otherwise} \end{cases}, \tag{16e}$$

$$\tilde{\mathcal{D}}^{j}_{k+1,[i]} := \hat{\boldsymbol{F}}^{j,-1}_{k+1}(\hat{\boldsymbol{F}}^{p(j)}_{k}\boldsymbol{d}^{p(j)}_{k} + (\hat{\boldsymbol{F}}^{j}_{k+1} - \hat{\boldsymbol{F}}^{p(j)}_{k})\hat{\mathcal{D}}^{j}_{k+1,[i]}), \tag{16f}$$

$$\breve{\boldsymbol{d}}^{j}_{k+1} = \sum_{i=1}^{2^{n_d}} \tilde{v}_i \tilde{\mathcal{D}}^{j}_{k+1,[i]}, \quad \sum_{i=1}^{2^{n_d}} \tilde{v}_i = 1, \tag{16g}$$

$$\breve{\boldsymbol{P}}^{j}_{k+1} = \textstyle\sum_{i=1}^{2^{n_d}} \tilde{v}_i\,(\tilde{\mathcal{D}}^{j}_{k+1,[i]} - \breve{\boldsymbol{d}}^{j}_{k+1})(\tilde{\mathcal{D}}^{j}_{k+1,[i]} - \breve{\boldsymbol{d}}^{j}_{k+1})^T, \tag{16h}$$

$$\tilde{\boldsymbol{P}}^{j}_{k+1} = \frac{1}{1-\chi^{j}_{k+1}}\breve{\boldsymbol{P}}^{j}_{k+1} + \frac{n_d\, F_{\text{dist}}(n_d, t-n_d, \alpha)}{\chi^{j}_{k+1}}\hat{\boldsymbol{F}}^{j,-1}_{k+1}, \tag{16i}$$

$$(\boldsymbol{d}^{j}_{k+1}, \boldsymbol{P}^{j}_{k+1}) = \mathbb{I}(\boldsymbol{d}^{p(j)}_{k}, \tilde{\boldsymbol{d}}^{j}_{k+1}, \boldsymbol{P}^{p(j)}_{k}, \tilde{\boldsymbol{P}}^{j}_{k+1}, \phi^{j}_{k+1}), \tag{16j}$$

$$\mathcal{D}^{j}_{k+1} = \mathbb{S}(\boldsymbol{d}^{j}_{k+1}, \boldsymbol{P}^{j}_{k+1}), \tag{16k}$$

The a-priori estimate of the FIM considering the future measurements ($\hat{\boldsymbol{F}}^{j}_{k+1}$) is obtained using (16a). An estimate of the future least-squares estimate is predicted by solving an approximate least-squares estimation problem as in (Thangavel et al., 2017) using (16b), where $\boldsymbol{d}^{p(j)}_{k}$ and $\hat{\boldsymbol{F}}^{p(j)}_{k}$ represents the approximate parameter estimate and its corresponding Fisher information matrix obtained if the state $\boldsymbol{x}^{p(j)}_{k}$ is considered as the plant measurement at time step k. An a posteriori estimate of the parameter covariance matrix considering the future measurements ($\tilde{\boldsymbol{P}}^{j}_{k+1}$) is obtained using (16i) taking into account the uncertainty in the predicted future parameter estimates. The key idea is to over-approximate the confidence region that was obtained at the previous time step using N_b boxes (as shown in Fig. 3 for a system with two uncertain parameters) and to handle each box in one of the scenarios as in Thangavel et al. (2017). The vertices of the box over-approximation of the confidence region ($\hat{\mathcal{D}}^{j}_{k+1}$) considered in a scenario j are obtained using (16c)–(16e) and are considered to be the candidate parameters that are realized in the future. The approximate least-squares estimate obtained if $\hat{\mathcal{D}}^{j}_{k+1}$ is realized at the next time step is given by (16f), $\forall i \in \{1, \cdots, 2^{n_d}\}$, where $\hat{\mathcal{D}}^{j}_{k+1,[i]}$ represents the i^{th} element of the set. The region which contains the future parameter estimates is approximated using an ellipsoid $\mathbb{D}(\breve{\boldsymbol{d}}, \breve{\boldsymbol{P}})$, where $\breve{\boldsymbol{d}}$ and $\breve{\boldsymbol{P}}$ are given by (16g) and (16h). The additional uncertainty in the parameter estimates due to the lack of future measurements is added to the confidence region of the uncertain parameter in (16i). It represents the ellipsoidal over-approximation of the Minkowski sum of ellipsoids (Kurzhanskiy and Varaiya, 2006). The ellipsoidal over-approximation of the intersection between the past and the future confidence region is given by (16j). ϕ^{j}_{k+1} and χ^{j}_{k+1} are degrees of freedom of the D-MS-SP NMPC optimization problem and are bounded between 0 and 1. The future parameter estimates that are considered to build the scenario tree of the D-MS-SP NMPC are given by (16k). After the robust horizon (i.e. $k \geq t + N_r$), the parameters considered to build the scenario tree are given by $\mathcal{D}^{j}_{k+1} = \mathcal{D}^{\lceil j/N_b \rceil}_{N_r-1}$.

7. CASE STUDIES

The performance of the different multi-stage control approaches is compared in two simulation studies. The first case study considers a linear model with a tracking objective whereas the second case study considers an exothermic semi-batch reactor (described by a nonlinear model) with an economic objective. The differential equations are discretized using orthogonal collocation on finite elements and the optimization problems are solved using IPOPT (Wächter and Biegler, 2006) with CasADi interface (Andersson et al., 2019). All the nodes in the scenario tree at time step k are equally weighted. The weights associated with the sigma points (v_i) are chosen as $[0\ 0.25\ 0.25\ 0.25\ 0.25]^T$ (i.e. weight associated with $\boldsymbol{d}_0$ is chosen as 0 and all the other sigma points are equally weighted).

7.1 Case Study 1: Linear system with tracking cost

We consider a system modelled as

$$\dot{x}_1 = p_1 u_1 - p_2, \tag{17}$$

$$\dot{x}_2 = p_2 u_2, \tag{18}$$

where x_1 and x_2 denote the model states with initial conditions $(0, 0)^T$ and are unconstrained. u_1 and u_2 represent

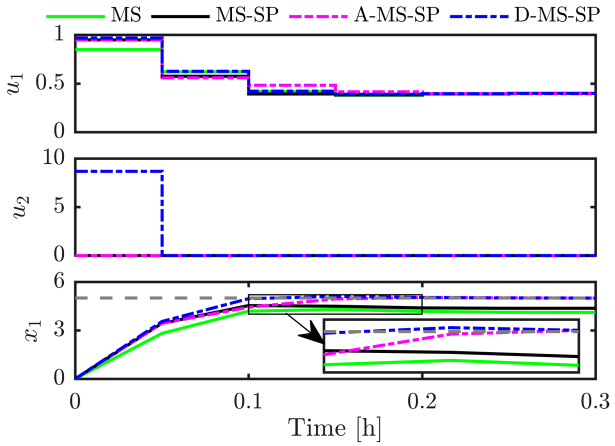

Fig. 4. Evolution of inputs (u_1, u_2) and state (x_1) under different MPC strategies (set point - grey dashed).

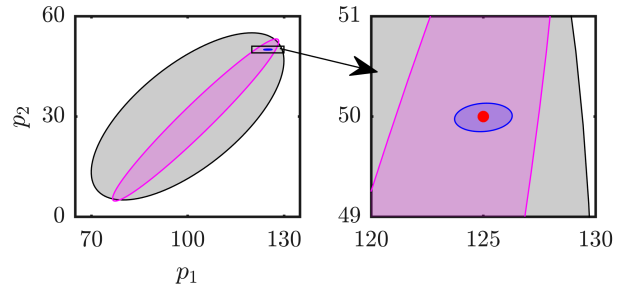

Fig. 5. Confidence region of the uncertain parameters for different MPC strategies at $t = 0.05\,\mathrm{h}$ (black - MS-SP MPC, magenta - A-MS-SP MPC, blue - D-MS-SP MPC, red dot - real value).

the control inputs and are bounded between 0 and 50. The measurement error bound is given as $(10^{-2}, 10^{-2})^T$. The objective of the controller is to track the state x_1 and is given by $J(\boldsymbol{x}, \boldsymbol{u}) = (x_1 - 50)^2 + \Delta u_1^2 + 10^{-4} u_2$, where Δ represents the deviation between successive control inputs. The sampling time is 0.05 h and the lengths of the prediction (N_p) and the robust horizons (N_r) are 10 and 2, respectively. The true values of the parameters $(p_1, p_2)^T = (125, 50)^T$ are unknown. The tuning parameter κ is chosen as 2. It was chosen such that (9) is satisfied based on a posterior analysis using simulation studies. The nominal value and the initial parameter covariance matrix of the uncertain parameters are given as

$$\boldsymbol{d}_0 = \begin{bmatrix} 100 \\ 30 \end{bmatrix}, \quad \boldsymbol{P}_0 = \begin{bmatrix} 900 & 500 \\ 500 & 625 \end{bmatrix}. \tag{19}$$

The results obtained using different MPC strategies and the confidence regions of the uncertain parameters that are considered at the first stage by the different MPC optimization problems solved at the second time step ($t = 0.05$) are shown in Figs. 4 and 5. The input u_2 does not have an influence on the state x_1 but provides more information about the uncertain parameter p_2 if $u_2 \neq 0$. Input u_2 is penalized in the cost function of the MPC, hence u_2 is always maintained at 0 using MS MPC or MS-SP MPC or A-MS-SP MPC as shown in Fig. 4. D-MS-SP MPC takes into account that u_2 can be used to improve the knowledge about p_2 which in turn can be used to improve the performance of the controller as shown in Fig. 4. MS MPC and MS-SP MPC do not reach the set point because of the large uncertainty in the parameters whereas A-MS-SP MPC and D-MS-SP MPC use the plant measurements to improve the knowledge about the uncertain parameters and reach the set-point.

It can be seen in Fig. 5 that the confidence region of the uncertain parameters obtained using D-MS-SP MPC is much smaller when compared to MS-SP or A-MS-SP MPC due to the probing input u_2. This results in D-MS-SP MPC reaching the set point faster when compared to the other MPC strategies. The cumulative objective until the final time obtained is 9.1 using MS MPC, 5.2 using MS-SP MPC, 3.9 using A-MS-SP MPC and 3.2 using D-MS-SP MPC. The sigma points tightly approximate the uncertainty region when compared to standard MS MPC hence MS-SP MPC outperforms MS MPC. A-MS-SP MPC uses the plant measurements to improve the knowledge about the uncertain parameters and performs better than MS-SP MPC. D-MS-SP MPC uses probing inputs to improve the knowledge about the uncertain parameters and outperforms all the other control schemes.

7.2 Case study 2: Nonlinear semi-batch reactor model with economic cost

The exothermic semi-batch reactor benchmark problem originally from (Srinivasan et al., 2003) and adapted as in (Thangavel et al., 2017) is chosen to show the advantages of the proposed scheme. The chemical reaction that takes place inside the reactor follows the reaction scheme $\mathrm{A} + \mathrm{B} \rightarrow \mathrm{C}$. The nonlinear model is obtained from the mass balance of the reactor with volume V_R, the molar balance of the reactants A and B with concentrations c_A and c_B, and the energy balances of the reactor and the jacket with temperature T_R and T_J. The dynamics of the semi-batch reactor is given by

$$\dot{V}_\mathrm{R} = u, \tag{20a}$$
$$\dot{c}_\mathrm{A} = -\frac{u}{V_\mathrm{R}} c_\mathrm{A} - K c_\mathrm{A} c_\mathrm{B}, \tag{20b}$$
$$\dot{c}_\mathrm{B} = \frac{u}{V_\mathrm{R}} (c_{\mathrm{B,\,in}} - c_\mathrm{B}) - K c_\mathrm{A} c_\mathrm{B}, \tag{20c}$$
$$\dot{T}_\mathrm{R} = \frac{u}{V_\mathrm{R}} (T_\mathrm{in} - T) - \frac{\alpha A_\mathrm{w} (T_\mathrm{R} - T_\mathrm{J})}{\rho V_\mathrm{R} c_p} - \frac{k c_\mathrm{A} c_\mathrm{B} H}{\rho c_p}, \tag{20d}$$
$$\dot{T}_\mathrm{J} = \frac{\dot{Q}_\mathrm{K} + \alpha A_\mathrm{w} (T_\mathrm{R} - T_\mathrm{J})}{\rho V_\mathrm{J} c_p}, \tag{20e}$$

with

$$c_\mathrm{C} = \frac{c_{\mathrm{A},0} V_{\mathrm{R},0} + c_{\mathrm{C},0} V_{\mathrm{R},0} - c_\mathrm{A} V_\mathrm{R}}{V_\mathrm{R}}, \tag{20f}$$
$$A_\mathrm{w} = \pi r^2 + \frac{0.002 V_\mathrm{R}}{r}, \tag{20g}$$

where c_C represents the concentration of the product C, with initial condition $c_{\mathrm{C},0}$ ($= 0\,\mathrm{mol/L}$), A_w denotes the surface of the reactor covered with the reaction mixture, α ($= 1.6 \times 10^3\,\mathrm{kJ/(K\,h\,m^2)}$) denotes the heat-transfer coefficient between the reactor and jacket, and r ($= 0.092\,\mathrm{m}$) denotes the radius of the cross-section of the reactor. The density ρ ($= 10^3\,\mathrm{g/l}$) and the specific heat capacity c_p ($= 4.2\,\mathrm{J/(g\,K)}$) are assumed to be constant. $c_{\mathrm{B,in}}$ ($= 3\,\mathrm{mol/l}$) and V_J ($= 2.22\,\mathrm{L}$) represent the input concentration of

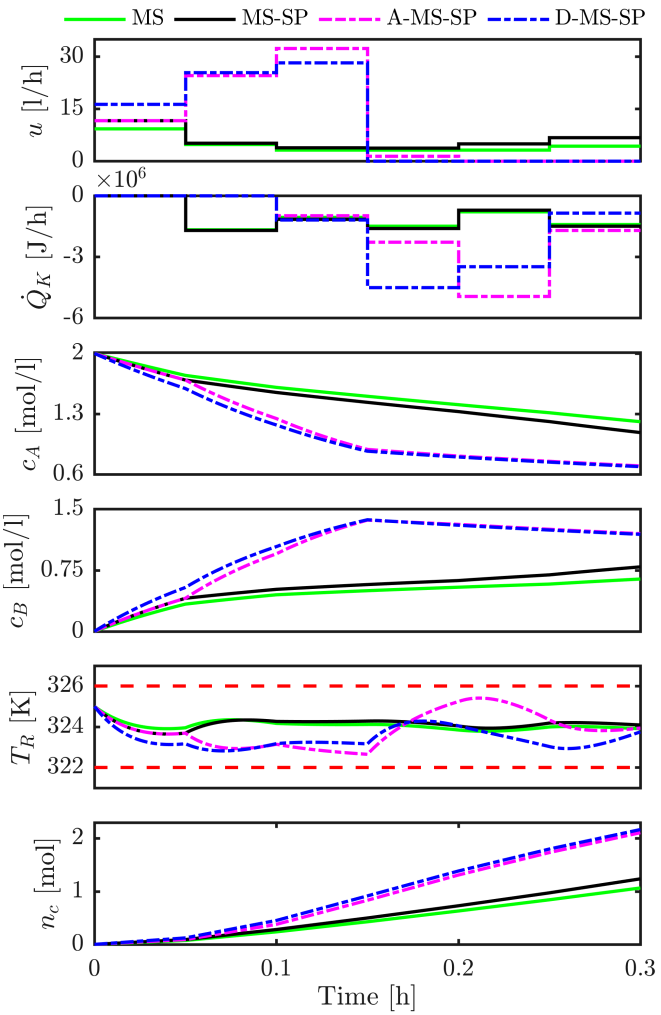

Fig. 6. Input feed, jacket cooling capacity and moles of product C obtained using different NMPC strategies.

reactant B and the volume of the cooling jacket. The reaction rate constant K and the reaction enthalpy H are uncertain parameters. The nominal values of the uncertain parameters and the initial parameter covariance matrix are

$$\boldsymbol{d}_0 = \begin{pmatrix} H \\ K \end{pmatrix} = \begin{pmatrix} -355\,\frac{\text{kJ}}{\text{mol}} \\ 1.205\,\frac{\text{L}}{\text{mol h}} \end{pmatrix}, \boldsymbol{P}_0 = \begin{pmatrix} 1.13 \times 10^4 & -7.7 \\ -7.7 & 0.131 \end{pmatrix}.$$

The control inputs are the feed rate $u \in [0, 32.4]$l/h and the cooling capacity $\dot{Q}_\text{K} \in [-9, 0] \times 10^3\,\text{kJ/h}$. The initial condition is given by $\boldsymbol{x}_0 = [V_{\text{R},0}\ c_{\text{A},0}\ c_{\text{B},0}\ T_{\text{R},0}\ T_{\text{J},0}]^T = [3.5\ 2\ 0\ 325\ 325]^T$. All states are assumed to be measured and the measurement vector is given as $\boldsymbol{y} = [V_\text{R}\ c_A\ c_B\ T_R\ T_J]^T$. The standard deviations of the measurement noises are given as $(0.0001, 0.01, 0.01, 0.1, 0.1)^T$. The sampling time of the NMPC is chosen as 0.05 h.

The control task is to maximize the number of moles (n_C) of product C produced along the prediction horizon while respecting tight constraints on the reactor temperature $322\,\text{K} \leq T_R \leq 326\,\text{K}$ and the volume constraint of the reactor $V_\text{R} \leq 7\,\text{L}$. The constraints are implemented as soft constraints. The robust horizon and the prediction horizon of the multi-stage NMPC are chosen as 2 and 5, respectively. The simulations are carried out until 0.3 h.

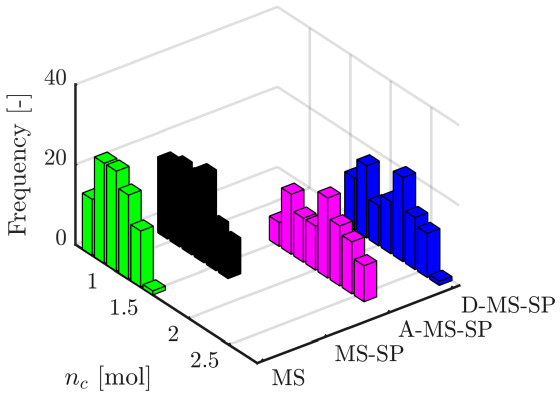

Fig. 7. Number of moles of product C produced by different robust NMPC strategies.

The tuning parameter κ is chosen as 1.70 and was obtained using trial and error.

The optimal operation is to feed as much reactant B as possible while respecting the constraints. MS NMPC feeds a small amount of reactant B because of the tight specification of the admissible reactor temperature and the presence of a large uncertainty in the parameters. The scenarios generated using the upper bound on the reaction enthalpy H and the lower bound on the reaction rate K hit the lower constraint on the reactor temperature, whereas the scenarios generated using the lower bound on the reaction enthalpy H and the upper bound on the reaction rate K hit the upper constraint on the reactor temperature in the predictions. This prevents standard MS NMPC from feeding more reactant into the reactor. MS-SP NMPC feeds more reactant B into the reactor because the sigma points approximate better the uncertainty set using its mean and variance in contrast to the traditional MS NMPC approach. There is a 16% increase in the number of moles of product C produced when using MS-SP NMPC over standard MS NMPC. The amount of the reactant fed into the reactor can be increased further using A-MS-SP and D-MS-SP NMPC because the scenario tree is continuously updated when better estimates of the uncertain parameters becomes available. In addition, D-MS-SP NMPC takes into account the future availability of measurement information and the possibility to adapt the scenario tree based on the predicted future confidence region along the prediction horizon. This implicitly takes into account the effect of probing control actions on the future confidence regions. The reactor is filled completely at 0.25 h and 0.2 h using the A-MS-SP and D-MS-SP NMPC. There is a 3% increase in the number of moles of product C produced when using the D-MS-SP NMPC over the A-MS-SP NMPC approach. The performance improvement is observed because the D-MS-SP NMPC considers the reduction in the range of the uncertainty due to the future measurements in its scenario tree.

In order to evaluate the performance of different NMPC strategies, the simulations were repeated for 100 random realizations of the uncertain parameters chosen within the initial confidence region of the uncertain parameter. Fig. 7 shows a histogram plot of the number of moles of product C produced. D-MS-SP NMPC outperforms the other NMPC strategies. There is a 16%, 68% and 2.5%

increase, in the number of moles of product C produced when using MS-SP NMPC over MS NMPC, A-MS-SP NMPC over MS-SP NMPC and D-MS-SP NMPC over A-MS-SP NMPC. The average computational times for one iteration of the MS, MS-SP, A-MS-SP and D-MS-SP NMPC approaches are 1.2 s, 0.7 s, 0.8 s, and 5.5 s. MS NMPC considers 9 scenarios at each node whereas all other NMPC approaches consider only 5 scenarios at each node. The increase in the computational complexity of A-MS-SP NMPC and D-MS-SP NMPC approach over MS-SP NMPC approach is due to the computation of the optimal over-approximation ellipsoid $\boldsymbol{P}_t$ in the NMPC optimization problem and the computation of future confidence regions of the uncertain parameters along the prediction horizon.

8. CONCLUSION

The proposed multi-stage NMPC variants using sigma point principles tightly over-approximate the uncertainty set and result in a better performance when compared to the traditional multi-stage NMPC approaches. The performance is further improved using an adaptive variant of the proposed scheme which uses the plant measurement to reduce the amount of uncertainty associated with the nominal model, and a dual variant which takes into account the future reduction in the uncertainty and the effect of future control actions on the shape of the future confidence region of the uncertain parameters. The future work will focus on improving the performance of the proposed MS-SP NMPC variants further by building the covariance matrix w.r.t. the uncertain parameters for the objective and constraint functions instead of the states.

REFERENCES

Andersson, J.A.E., Gillis, J., Horn, G., Rawlings, J.B., and Diehl, M. (2019). CasADi – A software framework for nonlinear optimization and optimal control. *Mathematical Programming Computation*, 11(1), 1–36.

Bargiela, A. (2001). *Interval and Ellipsoidal Uncertainty Models*, 23–57. Physica-Verlag HD, Heidelberg.

Farrokhsiar, M. and Najjaran, H. (2012). An unscented model predictive control approach to the formation control of nonholonomic mobile robots. In *2012 IEEE International Conference on Robotics and Automation*, 1576–1582.

Feldbaum, A.A. (1960). Dual control theory I. *Automation Remote Control*, 21, 874–880.

Filatov, N. and Unbehauen, H. (2000). Survey of adaptive dual control methods. *IEE Proceedings - Control Theory and Applications*, 147, 118–128.

Franceschini, G. and Macchietto, S. (2008). Model-based design of experiments for parameter precision: State of the art. *Chem. Eng. Sci.*, 63(19), 4846–4872.

Heine, T., Kawohl, M., and King, R. (2006). Robust model predictive control using the unscented transformation. In *2006 IEEE Conference on Computer Aided Control System Design, 2006 IEEE International Conference on Control Applications, 2006 IEEE International Symposium on Intelligent Control*, 224–230.

Julier, S.J. (2002). The scaled unscented transformation. In *P AMER CONTR CONF*, volume 6, 4555–4559.

Julier, S. and Uhlmann, J. (1997). A new extension of the kalman filter to nonlinear systems. In *Proc. of AeroSense: The 11th Int. Symp. on Aerospace/Defense Sensing, Simulations and Controls*.

Kurzhanskiy, A.A. and Varaiya, P. (2006). Ellipsoidal toolbox (et). In *Proceedings of the 45th IEEE Conference on Decision and Control*, 1498–1503.

Lucia, S., Finkler, T., Basak, D., and Engell, S. (2012). A new robust nmpc scheme and its application to a semi-batch reactor example. *IFAC Proceedings Volumes*, 45(15), 69 – 74. 8th IFAC Symposium on Advanced Control of Chemical Processes.

Lucia, S., Finkler, T., and Engell, S. (2013). Multi-stage nonlinear model predictive control applied to a semi-batch polymerization reactor under uncertainty. *J Process Contr*, 23, 1306–1319.

Mayne, D., Seron, M., and Rakovic, S. (2005). Robust model predictive control of constrained linear systems with bounded disturbances. *Automatica*, 41, 219 – 224.

Mesbah, A. (2018). Stochastic model predictive control with active uncertainty learning: A survey on dual control. *Annual Reviews in Control*, 45, 107 – 117.

Scokaert, P. and Mayne, D. (1998). Min-max feedback model predictive control for constrained linear systems. *IEEE Transactions on Automatic Control*, 43(8), 1136–1142.

Srinivasan, B., Palanki, S., and Bonvin, D. (2003). Dynamic optimization of batch processes: I. Characterization of the nominal solution. *Computers & Chemical Engineering*, 27(1), 1–26.

Thangavel, S., Lucia, S., Paulen, R., and Engell, S. (2017). Robust nonlinear model predictive control with reduction of uncertainty via dual control. In *2017 21st International Conference on Process Control (PC)*, 48–53.

Thangavel, S., Lucia, S., Paulen, R., and Engell, S. (2018a). Dual robust nonlinear model predictive control: A multi-stage approach. *Journal of Process Control*, 72, 39 – 51.

Thangavel, S., Paulen, R., and Engell, S. (2020b). Adaptive multi-stage NMPC using sigma point principles. In *2020 19th European Control Conference (ECC)*.

Thangavel, S., Aboelnour, M., Lucia, S., Paulen, R., and Engell, S. (2018b). Robust dual multi-stage nmpc using guaranteed parameter estimation. *IFAC-PapersOnLine*, 51(20), 72 – 77.

Thangavel, S., Paulen, R., and Engell, S. (2020a). Multi-stage NMPC using sigma point principles. *IFAC Conference on Advances in Control & Optimization of Dynamical Systems (ACODS), Chennai*.

Thangavel, S., Subramanian, S., and Engell, S. (2019). Robust nmpc using a model-error model with additive bounds to handle structural plant-model mismatch. 12th IFAC Symposium on Dynamics and Control of Process Systems.

Thangavel, S., Subramanian, S., Lucia, S., and Engell, S. (2018c). Handling structural plant-model mismatch using a model-error model in the multi-stage NMPC framework. *IFAC-PapersOnLine*, 51(15), 1074 – 1079.

Völz, A. and Graichen, K. (2015). Stochastic model predictive control of nonlinear continuous-time systems using the unscented transformation. In *2015 European Control Conference (ECC)*, 3365–3370.

Wächter, A. and Biegler, L. (2006). On the implementation of a primal-dual interior point filter line search algorithm for large-scale nonlinear programming. *Math Program*, 106, 25–57.

Wan, E.A. and Van Der Merwe, R. (2000). The unscented kalman filter for nonlinear estimation. In *Proceedings of the IEEE 2000 Adaptive Systems for Signal Processing, Communications, and Control Symposium*, 153–158.

Wittenmark, B. (1995). Adaptive dual control methods: An overview. In *Proc. of the 5th IFAC Symposium on Adaptive Systems in Control and Signal Processing*.

Yan, J. and Bitmead, R.R. (2005). Incorporating state estimation into model predictive control and its application to network traffic control. *Automatica*, 41(4), 595 – 604.